Measurement of nanometer-thick lubricating films using ellipsometric microscopy

Kenji Fukuzawa[1)*], Yusuke Sasao[1)], Katsuya Namba[1)], Chihiro Yamashita[1)], Shintaro Itoh[1)], and Hedong Zhang[2)]

[1)] Department of Micro/Nano Systems Engineering, Nagoya University,

Furo-cho, Chikusa-ku, Nagoya, 464-8603, Japan

[2)] Department of Complex Systems Science, Nagoya University,

Furo-cho, Chikusa-ku, Nagoya, 464-8603, Japan

[*]Corresponding author: fukuzawa@nuem.nagoya-u.ac.jp

Abstract

A method based on vertical-objective-based ellipsometric microscopy (VEM) is presented for measuring lubricant film thickness in nanometer sliding gaps. It provides an image of nanometer-thick lubricating films in real time at high lateral and thickness resolutions without any special layers. The ellipsometric image is directly converted into the film image by using a piezo-stage displacement method combined with a rotating compensator ellipsometry method. The accuracy of thickness measurement is about 1 nm. The VEM-based method revealed that nanometric deformation of the sliding surfaces arises in nanometric gaps even if the load is low, which significantly affects the lubrication properties in small gaps. This method is useful for clarifying the lubrication phenomena in nanometric sliding gaps.

1. Introduction

Along with progress in processing technology, narrower sliding gaps are needed to improve the performance of advanced machines, which requires more precise lubrication technology for the narrower gaps or the lubrication with very thin lubricant films [1], [2]. For example, the gaps between the head and disk in computer hard disk drives are now of the order of 1 nm. In addition, since reducing lubricant viscosity can meet social demands for energy saving, the lubrication in small gaps has attracted much attention, such as lubrication with lower viscosity lubricants for automotive engines. However, the lubrication in nanometric sliding gaps has not been fully established yet, because liquids that confined in nanometric gaps exhibit properties different from those of the bulk [3]-[7].

Measurement of gap shapes or thickness distribution of lubricating film is essential for clarifying the lubrication phenomena in small gaps. Optical-interferometry-based methods have been widely used for this purpose and have provided fruitful results in elastohydrodynamic lubrication in which sliding gaps or film thicknesses are more than about 100 nm; however, the sensitivity of such methods is too low for nanometer-thick film in principle. Since the difference in the light path length is needed to be at least half of the wavelength to give rise to optical interference, it is difficult to measure film thickness less than one-quarter wavelength of the light. If a typical visible light (wavelength of 500-600 nm) is used, the one-quarter wavelength is around 100 nm. That is why the measurement of film thickness less than about 100 nm is difficult for conventional optical interferometry.

A number of methods have been proposed to overcome this problem. One method, which is called spacer-layer imaging or ultra-thin film interferometry, uses a spacer layer consisting of a transparent layer such as a silica layer and a semi-reflective layer such as a thin chromium layer [8]-[9]. The sliding surface is coated with a spacer layer to elongate the light path. Thickness of the transparent silica layer is needed to adjust so that its optical path length is equal to the one-quarter wavelength. Another method, which is called relative optical interference intensity method, coats the sliding surfaces with a semi-reflective metal film such as a thin chromium layer [6]. This semi-reflective

metal film shifts the phase of the light that reflected from the sliding gap, and increases the sensitivity. In the former method, the test sliding surface is needed to be coated with a multilayer film (spacer layer). In the latter method, since the measurement accuracy significantly depends on optical properties of the semi-reflective chromium layer, the precise control of the thickness and refractive index of the chromium layer is needed [10], [11]. In Ref. [11], it was reported that a thickness of the chromium layer is needed to be 5 nm for precise thickness measurement. Thus, both methods require coating of test sliding surfaces with precisely-controlled special layers, which limits variety of test sliding surfaces and makes test surfaces different from practical ones.

Ellipsometry is widely used for measuring the thickness of thin films on substrates without any modification of the samples, such as adding the special layer. Ellipsometers can provide the thickness of nm-thick films at a single sample point at a thickness resolution of 0.1 nm or less [12], [13]. Aimed at improvement in the measurement speed, ellipsometric microscopy (EM), or imaging ellipsometry, uses an imaging device such as a CCD camera instead of a photodetector [14], [15]. Such methods could provide the thickness distribution at a time as an image; however, they have low lateral resolution. Oblique illumination is needed to obtain ellipsometric signal as in conventional ellipsometers. Conventional ellipsometric microscopes use oblique observation corresponding to the oblique illumination. In this setup, the focal plane of the objective lens is not normal to the sample plane, which narrows the focus region. This problem is more serious when a higher resolution lens is used. For example, the focus region is only about 1 μm when an objective lens with a numerical aperture of 0.9 is used. Therefore, the lateral resolution is larger than about 10 μm.

Vertical-objective-based EM (VEM) improves the lateral resolution [16]-[20]. A lateral resolution of 0.1 μm order was achieved for thickness measurement of thin films coated on substrates by combining vertical observation with off-axis Kőhler illumination. It was demonstrated that this VEM can visualize nm-thick solid thin films [16], [17] and nm-thick liquid thin films in real time [18]-[20]. In this paper, we first proposed a method that applies VEM to measurement of nanometric lubricant thickness in sliding gaps, which does not require special layers such as spacer layers and semi-reflective chromium layer. This VEM-based method can provide real-time imaging of

lubricating film in nm-sliding gaps at high lateral resolution along with high thickness resolution.

2. Film thickness measurement method based on ellipsometric microscopy

2.1 VEM-based measurement of lubricating film thickness

Figure 1 shows a schematic setup of film thickness measurement based on VEM. As shown in Fig. 1(a), setting the observation system vertical to the sample surface can provide diffraction-limited lateral resolution of the order of 0.1 μm. Oblique illumination is needed to obtain an ellipsometric signal as with conventional ellipsometers. To achieve this in VEM while remaining compatible with the vertical observation system, the illumination light is focused onto an off-axis point on the back focal plane of the objective lens as shown in Fig. 1(b). This enables oblique and parallel light illumination to be generated, and provides a sufficient ellipsometric signal. Since our method is based on ellipsometry, it has sufficient sensitivity for nanometer-thick lubricating films. In addition, it enables the films to be visualized in real time.

In this measurement, a plano-convex glass lens was used as the slider to make the surface smooth on the nm scale, and the lens surface was coated with a metal layer (stain-less steel layer) to simulate the practical surfaces. Note that this metal coating layer does not require special adjustment for improvement of measurement accuracy, unlike the spacer-layer and semi-reflective layer that described in Section 1. Therefore, for example, a steel ball with a smooth surface can be used as the slider. A glass plate was used as the substrate, as shown in Fig. 1. The light from the light source was reflected at the gap between the metal-coated lens and sliding glass substrate, which is filled with the lubricant. If the amplitude reflectivity ratio of the p- and s-polarization lights are r_p and r_s, respectively, the complex reflectivity ratio of p- and s-polarization lights, ρ, is given by [12]

$$\rho = \frac{r_p}{r_s} = \tan\Psi(h)e^{i\Delta(h)}, \tag{1}$$

where $\tan\Psi$ and Δ are defined as the absolute value and argument of reflectivity ratio ρ, respectively.

Since ρ changes with lubricating film thickness h, the intensity of the reflected light from the gap reflects film thickness h; therefore, film thickness h can be obtained by analyzing the intensity of images obtained by VEM, called “ellipsometric images” here.

2.2 Conversion of ellipsometric image to lubricating film image

Direct conversion from the image intensity to the film thickness was attempted. Direct conversion enables acquisition of the film image at a high frame rate, which can be equal to the maximum frame rate of the imaging device. The conversion curve or the relationship between the image intensity and film thickness is needed. This calibration requires a sample with known film thicknesses or gaps. As shown in Fig. 2(b), a simple approach is to prepare different gap filled with the lubricant by changing the separation between the lens and substrate with a precise drive mechanism such as a piezo stage. With this approach, the physical quantity obtained is the stage displacement, which is not the gap or film thickness but its change. A contact point can be used to convert the displacement into the film thickness. At the points of contact between the lens and substrate, the film thickness is equal to zero; therefore, the piezo displacement at the contact point gives the difference between the displacement and film thickness. However, the gap around the contact point is generally difficult to obtain precisely by using piezo displacement, because the contact surfaces generally deform due to adhesion on the nm-scale. Therefore, another approach was introduced to measure the gap or film thickness around the contact point.

A rotating compensator ellipsometry (RCE)-based method was introduced for measuring the film thickness around the contact point. For larger thicknesses, the image intensity was measured while changing the thickness or gap by moving the piezo stage, and the relationship between the image intensity and piezo displacement was obtained. The data obtained from the two measurements were merged, and a conversion curve was obtained so as to minimize the error between the merged data and fitting curve. The details of this method are described here.

Figure 2(a) illustrates RCE-based measurement of the film thickness around the contact point. In this measurement, the lens is brought into contact with the glass substrate. The various film

thicknesses are formed around the contact region such as h_1 and h_2 in Fig. 2(a). The ellipsometry image intensity at each sample point is measured while rotating the compensator in the VEM. Here, the angles of the polarizer and analyzer were respectively set at 0 and 45 degrees with respect to the p-polarization direction. The ellipsometry image intensity I at a compensator angle C is given by [12]

$$I(C) = I_0 \frac{|r_s|^2}{\cos^2 \Psi} (\alpha_4 \cos(4C) + \beta_2 \sin(2C) + \beta_4 \sin(4C)), \tag{2}$$

where

$$\beta_2 = -2 \sin 2\Psi \sin \Delta,\ \alpha_4 = -\cos 2\Psi,\ \beta_4 = \sin 2\Psi \cos \Delta. \tag{3}$$

I_0 is the intensity of the illumination light, and r_s is the amplitude reflectivity for the s-polarized light. Using Eq. (3), we can obtain Ψ and Δ from coefficients β_2, α_4, and β_4.

Coefficients β_2, α_4, and β_4 are experimentally obtained by capturing the lubricating film images synchronously with the rotation of the compensator. The exposure time of the imaging device is set to t_{exp}. If a CCD camera is used as the imaging device, the image intensity at each pixel is integrated during t_{exp}. If t_{exp} is set to $T/16$, where T is the period per rotation of the compensator, the integrated intensity at each exposure is equal to the area of regions I_1 to I_{16} in Fig. 3. Thus, 16 images are captured during one rotation, and the integrated image intensities at each pixel are equal to the areas of I_1 to I_{16}. Since Eq. (2) is a periodic function of compensator angle C, the coefficients in Eq. (2) can be obtained from the areas of the 16 regions in Fig. 3 [13].

$$\begin{aligned}
\beta_2 &= I_1 + I_2 + I_3 + I_4 - I_5 - I_6 - I_7 - I_8 + I_9 + I_{10} + I_{11} + I_{12} - I_{13} - I_{14} - I_{15} - I_{16} \\
\alpha_4 &= I_1 - I_2 - I_3 + I_4 + I_5 - I_6 - I_7 + I_8 + I_9 - I_{10} - I_{11} + I_{12} + I_{13} - I_{14} - I_{15} + I_{16} \\
\beta_4 &= I_1 + I_2 - I_3 - I_4 + I_5 + I_6 - I_7 - I_8 + I_9 + I_{10} - I_{11} - I_{12} + I_{13} + I_{14} - I_{15} - I_{16}.
\end{aligned} \tag{4}$$

Thus, Ψ and Δ are obtained from 16 images by VEM using Eqs. (3) to (4).

The VEM includes mirrors and lenses, which add errors (Ψ_e, Δ_e) to the measured values. These errors were determined by the method described below. First, ellipsometric angles when the lens and substrate made contact without lubricant, Ψ_{m0} and Δ_{m0}, are measured by VEM. In this measurement, the entire lens surface in the field of view of the microscope is brought into contact with the substrate by applying a large load. This means that the film thickness at all point in the ellipsometric image is set at 0. Next, the theoretically predicted (Ψ_{t0}, Δ_{t0}) at a thickness of 0 are calculated. (Ψ_{t0}, Δ_{t0}) are obtained by substituting the respective refractive indexes of a glass substrate (N_0) and a meal-coated lens (N_2) and into Eqs. (5) and (6), which is based on a two layer model (metal /glass substrate) [12]:

$$\tan\Psi_{t0}\exp(i\Delta_{t0}) = \frac{r_{02p}}{r_{02s}} \tag{5}$$

$$\text{where } r_{02p} = \frac{N_2\cos\theta_0 - N_0\cos\theta_2}{N_2\cos\theta_0 + N_0\cos\theta_2}, r_{02s} = \frac{N_0\cos\theta_0 - N_2\cos\theta_2}{N_0\cos\theta_0 + N_2\cos\theta_2}. \tag{6}$$

Subscripts s and p indicate s- and p-polarized lights, respectively. The difference between the measured (Ψ_{m0}, Δ_{m0}) and theoretically predicted (Ψ_{t0}, Δ_{t0}) are considered to be the errors (Ψ_e, Δ_e). In the measurements of the thickness of lubricating films, the errors (Ψ_e, Δ_e) at each point of the sample are removed from the measured values (Ψ_m, Δ_m).

From the measured angles (Ψ_m, Δ_m) for a sample gap filled with lubricant, film thickness h is obtained so as to minimize the error between the theoretically calculated angles ($\Psi(h)$, $\Delta(h)$) and measured angles (Ψ_m, Δ_m) [20]. The theoretical angles ($\Psi(h)$, $\Delta(h)$) are obtained by using Eqs. (7) and (8), which is based on a three-layer model (metal/lubricant/glass substrate) [12]:

$$\begin{aligned}&\tan\Psi(h)\exp(i\Delta(h))\\ &= \frac{r_{01p} + r_{12p}\exp(-2id)}{1 + r_{01p}r_{12p}\exp(-2id)} \times \frac{1 + r_{01s}r_{12s}\exp(-2id)}{r_{01s} + r_{12s}\exp(-2id)},\end{aligned} \tag{7}$$

$$\text{where } d = 2\pi N_1 h\cos\theta_1/\lambda,\ r_{ijp} = \frac{N_j\cos\theta_i - N_i\cos\theta_j}{N_j\cos\theta_i + N_i\cos\theta_j}, r_{ijs} = \frac{N_i\cos\theta_i - N_j\cos\theta_j}{N_i\cos\theta_i + N_i\cos\theta_i}(i,j = 0,1,2). \quad (8)$$

Here, N_1 is the refractive index of the lubricant, and λ is the wavelength of the light. The conversion curve is obtained by measuring the ellipsometric image intensity and film thickness using the RCE-based method for the same point on the sample.

Figure 2(b) shows the piezo-stage-based calibration method used for larger film thickness. The ellipsometric image intensity is measured while separating the lens from the glass substrate by moving the piezo stage. The relationship between the ellipsometric image intensity and the displacement of the piezo stage is obtained. Here, the compensator angle was fixed at 60 deg. As described above, the displacement of the piezo stage is the change in the gap or film thickness. The displacement is shifted from the true thickness by an unknown amount h_p. To determine h_p, the data obtained using the piezo method and RCE method are merged, and fitted to a quadratic function. A quadratic function is used because the theoretical curve can be well fitted by a quadratic function as shown in Fig. 4(b). The data obtained by the piezo method is shifted in the horizontal direction so as to minimize the difference between the merged data and fitting curve, and the conversion curve is obtained.

3. Materials and methods

Poly-α-olefin (PAO) was used as the sample lubricant; its viscosity was about 0.07 Pa s, and its refractive index was 1.46. A high-refractive index glass (K-LASFN23) was used as the substrate; its refractive index is 1.94 according to the manufacturer (Sumita Optical Glass, Japan). Its thickness was 0.8 mm. The lens consisted of BK7 glass, and its radius of curvature was 15.6 mm. Only the lens was coated with 53-nm-thick stainless-steel film by sputtering. The refractive index of the stainless-steel film on the flat glass substrate, as measured with a commercial spectroscopic ellipsometer (FE-5000S, Otsuka Electronics, Japan), was 1.43-2.60*i*. The surface roughness of the

metal-coated lens and substrate were measured with an atomic force microscope (Icon, Bruker, USA); the R_a of the lens and substrate were 0.7 and 0.3 nm, respectively.

A modified inverted optical microscope (IX-71, Olympus, Japan) was used for the VEM, as shown in Fig. 1. The numerical aperture of the objective lens was 0.8 (M Plan 100 PC, Nikon, Japan). This objective lens enabled us to observe the lubricating film through the glass substrate whose thickness is around 1 mm. The incident angle was set to be 35 deg, which was limited by the aperture size of the lens. A polarizer, compensator (quarter-wave plate), and analyzer were added to the microscope. An LED with a wavelength of 460 nm (X-Cite, Lumen Dynamics, USA) was used as the light source, and a highly sensitive electron-multiplying CCD camera (Cascade II, Photometrics, USA) was used as the detector. All images of the lubricating film were the averaged image of 50 images except in the RCE-based calibration. The five images were averaged to obtain the area of regions I_1 to I_{16} in Fig. 3.

A sliding mechanism was built up on the sample stage of the microscope. A metal-coated lens was attached to the double cantilever, and the load was obtained by multiplying the spring constant by the displacement of the double cantilever measured with a spectral interference sensor (SI-F1000V, Keyence, Japan). The glass substrate was horizontally vibrated by the *x*-piezo stage (P-733.2DD, Physik Instrumente, Germany). The gap was adjusted by the *z*-piezo stage using displacement feedback from a capacitive sensor (P-753, Physik Instrumente, Germany). The displacement resolution of this stage is 0.05 nm. In this experiment, we did not measure the temperature near the contact area.

After the conversion curve was obtained as described in Section 2.2, the lubricating film image was obtained by converting the ellipsometric image intensity into the lubricating film image. Besides the terms shown in Eq. (2), the measured ellipsometric image intensity I includes background noise I_b, which is independent of both light intensity I_0 and thickness h. In addition, I_0 includes the unevenness of the illumination light intensity. Letting the measured image intensities when the thickness are 0 and h be I_{h0} and I_h, respectively, and with consideration of the noises, Eq. (2) for a film thickness of 0 and h can be respectively rewritten as

$$I_{h0} = I_b + I_0 I_n(0),$$
$$I_h = I_b + I_0 I_n(h). \tag{9}$$

where $I_n(h)$ is the normalized true image intensity, which does not have any noise. To obtain $I_n(h)$, measured image intensity I was processed using

$$I_p = \frac{I_h - I_{h0}}{I_{h0} - I_b} = \frac{I_n(h) - I_n(0)}{I_n(0)}. \tag{10}$$

I_b was obtained as the image when the light source was switched off. I_p is used in the discussion below, instead of measured intensity I.

In the measurement of the film thickness, the glass substrate was vibrated sinusoidally by the x-piezo stage at an amplitude of 15 μm and a frequency of 9.99 Hz (Fig. 1). The maximum sliding speed was 0.94 mm/s. The sliding speed during the sliding changed with time. Therefore, stroboscopic image capture was introduced in which the light source LED emitted the illumination light synchronously with the sliding, and the lubricating film image was captured only at a specific timing. An image of the lubricating film was captured at the maximum speed with a light pulse width of 1.8 ms.

4. Results and discussion

4.1 Conversion of ellipsometric image to lubricating film image

Figure 4(a) shows the obtained conversion curve. Blue and red circles represented data obtained by RCE and piezo methods. The intensity was averaged over a circular area with a diameter of 9.8 μm at the center of the lens. The thick black line is the obtained fitting curve, which is used to convert the ellipsometric image into a lubricating film image.

Figure 4(b) compares the conversion curve with the theoretically predicted one. The black line is the experimental one shown in Fig. 4(a). The theoretical curve was calculated using Eqs. (2), (3), (7), and (8). The refractive indexes of the glass substrate, lubricant, and stainless steel film (metal on lens) were set at the values as described in Section 3. $\Psi(h)$ and $\Delta(h)$ were calculated using Eqs. (7) and (8), and intensity I was obtained by substituting $\Psi(h)$ and $\Delta(h)$ into Eqs. (2) and (3). The good agreement between the experimental and theoretical curves indicates the validity of our conversion method.

4.2 Measurement of film thickness during static contact

Figure 5 shows the results of the static contact between the metal-coated lens and substrate, which was filled with lubricant. Using the Z-piezo stage as shown in Fig. 1, the lens was pressed against the substrate. The distribution of the film thickness was measured with VEM in the manner as described above. The red dots show the measured film thickness profile on the center line. The film thickness averaged over a 1.3-μm-wide area is shown.

The blue line shows the theoretical curve predicted by Hertzian contact theory [21]. In the theoretical calculation, the Young moduli of the lens and substrate were set to 79.9 and 124.9 GPa and the Poisson ratio was set to 0.209 and 0.295, respectively, in accordance with the manufacturer's instruction (Sumita Optical Glass, Japan). The load was adjusted so as to make the contact area equal to the experimental one. The estimated load was 40 mN.

The measured film profile shows good agreement with the theoretical one over the measurement range. This supports the validity of our conversion method. The standard deviation from 0 in the contact area at the center of the image was 1.2 nm, which is equal to the accuracy of the measurement.

4.3 Measurement of lubricating film by VEM

Figures 6 to 8 show the lubricating film measured during sliding by VEM. Figures 6 (a) and (b) show the contour map of the film thickness at a load of 1.7 mN and 8.5 mN, respectively. They are

shown at an interval of 2.5 nm. The film thickness image at maximum speed were captured using the stroboscopic imaging. The large bold arrows show the lubricant flow direction (*x*-direction). The film thickness was smaller at the higher load. The method could detect this difference on the order of 1 nm, as evidenced by these images.

Figures 7(a) and (b) show cross sectional views of Fig. 6(a) (load of 1.7 mN) on the center line in the *x*- and *y*-directions, respectively. The film thicknesses were averaged over a 3.6-μm-wide area. The blue lines represent the theoretical film thickness between the plane and a sphere as the same diameter as the metal-coated lens as a guide for the eye. The part of the film profile, in which the sliding surface was undeformed, closely matched the gap between the plane and sphere. This also supports the validity of our method. In the results shown in Figs. 6(a) and 7, the nm-scale deformation of the sliding surface on the inlet side was asymmetric in the lubricant flow direction (*x*-axis) and the film thickness was larger on the inlet side whereas that in the direction normal to the lubricant flow (*y*-axis) was symmetric. These results suggest that hydrodynamic pressure was generated by the sliding at these small gaps (less than 10 nm), and this pressure gave rise to nanometric deformation of the sliding surfaces.

Figures 8(a) and (b) show cross sectional views of Fig. 6(b) (load of 8.5 mN) on the center line. In order to clarify lubrication mode, assuming that the region that deviated from the gap shape between the sphere and substrate was almost flat, we roughly estimated the pressure of the region from the results shown in Figs. 6(b) and 8. Since its rough size was about 20 x 20 μm^2, the value of the average pressure in this region was estimated to be about 6.8 MPa by dividing the load by the area. At this load, Greenwood and Johnson's elasticity and viscosity parameters (g_E and g_V) were estimated to be 123 and 103, respectively [22], [23]. This indicates that the lubrication mode in these experiments was fluid lubrication without elastic deformation of the sliding surfaces and viscosity changes due to the pressure (isoviscous and rigid region). Application of Kapitza's equation to the data obtained in this experiment [24] gave estimated minimum film thicknesses of 180.6 nm and 7.2 nm at loads of 1.7 and 8.5 mN, respectively. In contrast, the experimental thicknesses at loads of 1.7 and 8.5 mN were 5.3 and 2.9 nm, respectively. These results demonstrate that conventional

lubrication theory is not applicable to the lubrication in nanometric gaps. In particular, nanometric elastic deformations of the sliding surfaces arose even when the loads were low. Although these deformations were small, they must have significantly affected the lubrication in nanometric sliding gaps because the deformation was comparable to the gap. The difference between the theoretical and experimental thicknesses may have been caused by the properties of the confined lubricants. In this experiment, reciprocating sliding was used. Since the relaxation time of a confined liquid is much longer than that of a bulk one, the slow relaxation may have caused smaller film thickness due to decreasing of the hydrodynamic pressure.

Thus, the nanometric deformations of the sliding surfaces along with the properties of confined lubricants should be considered when investigating the lubrication in nanometric small gaps. Our proposed method will thus be useful for clarifying the lubrication phenomena in nanometric sliding gaps.

It should be noted that surface roughness of the sliding surfaces affects the accuracy of ellipsometry because ellipsometry basically premises smooth surfaces as the optical-interferometry techniques. In this experiment, the surface roughness was much smaller than the wavelength; therefore, it can be thought that the influence of the roughness was negligibly small. The results that shown in Figs. 4 and 5 support the validity of this assumption. It was reported that surfaces with a roughness of less than one tenth of the wavelength of the light, which is around 50 nm for visible lights, can be treated as flat surfaces using an effective medium approximation [13], [25]. Rougher surfaces than that used in this experiment may require modification of the theory that considers the roughness effect.

In this experiment, the thickness of the glass substrate t_s was 0.8 mm. The thickness of the substrate was limited up to about 1 mm by the working distance of the used objective lens (Fig. 1). This limitation requires adjustment of the dimensions of the substrate and lens for high-pressure contact experiments by VEM such as those for elasto-hydrodynamic lubrication that done by interferometry techniques [6], [8]-[11]. For example, when the radius and thickness of circular substrate are respectively set at r_s = 2.5 mm and t_s = 1.0 mm, and the radius of curvature of the lens is set at 0.5 mm, the maximum pressure and radius of the contact area are estimated at 2.5 GPa and 43 μm for a

load P = 10 N, respectively, using Hertzian contact theory [21]. VEM can image the contact area in terms of its field of view. Moreover, the deflection of the substrate w_s is estimated at 0.11 μm if the load is concentrated onto the center of the substrate ($w_s = Pr_s^2/16\pi D$ where $D = E_s t_s^3/12(1-\nu_s^2)$, E_s: Young's modulus, ν_s: Poisson's ratio of the substrate) [26]. This deflection is smaller than the depth of field of VEM d_f, which was estimated at 0.36 μm for this setup ($d_f = \lambda/2NA^2$, NA: numerical aperture of the objective lens); therefore, it does not affect observation by VEM.

5. Summary

We have developed a method based on vertical-objective-based ellipsometric microscopy for measuring lubricant films in nm sliding gaps without any special layers, and demonstrated its feasibility. Direct conversion from an ellipsometric image into the film thickness by using the piezo stage method combined with the RCE method, enables to provide thickness measurement accuracy of about 1 nm. The measurement of the film thickness using this method indicated that nanometric deformation of the sliding surfaces arises in lubrication in nanometric sliding gaps, which significantly affects the lubrication properties of small gaps. Our proposed method is thus useful for clarifying lubrication phenomena in nanometric sliding gaps.

6. Acknowledgments

The authors wish to acknowledge Professor Umehara for his help in the measurement with a spectroscopic ellipsometer. This work was supported in part by the Advanced Storage Research Consortium and JSPS KAKENHI Grants of 26249013 and 17H01243.

References

[1] Dowson D. Developments in lubrication—The Thinning Film. J. Phys D 1992; 25: A334–9.

[2] Spikes H. Tribology Research in The Twenty-First Century. Tribol. Int. 2001; 34:12-789.

[3] Granick S. Motions and Relaxations of Confined liquids. Science 1991; 253-1374.

[4] Luengo G, Schmitt FJ, Hill R, Israelachvili J. Thin Film Rheology and Tribology of Confined Polymer Melts: Contrasts with Bulk Properties. Macromolecules 1997; 30: 8-2482.

[5] Israelachvili J. Thin Film Studies Using Mutiple-Beam Interferometry. J. Colloid Interface Sci. 1973; 44- 2259.

[6] Luo J, Wen S, Huang P. Thin film lubrication Part I: Study on the transition between EHL and thin film lubrication using a relative optical interference intensity technique. Wear 1996; 194-107.

[7] Matsuoka H, Kato T. An ultrathin liquid film lubrication theory—Calculation method of solvation pressure and its application to the EHL problem. J. Tribol. 1997; 119: 1-217.

[8] Johnston GJ, Wayte R, Spikes HA. The Measurement and Study of Very Thin Lubricant Films in Concentrated Contacts. Tribol. Trans. 1991; 34: 2-187.

[9] Glovnea RP, Forrest AK, Olver AV, Spikes HA. Measurement of sub-nanometer lubricant films using ultra-thin film interferometry. Tribol. Lett. 2003; 15: 3-217.

[10] Guo F, Wong PL. A multi-beam intensity-based approach for lubricant film measurements in non-conformal contacts. Proc. I. Mech. E. 2002; J216-281.

[11] Liran M, Zhang C, Discussion on the Technique of Relative Optical Interference Intensity for the Measurement of Lubricant Film Thickness. Tribol. Lett. 2009; 36-239.

[12] Azzam RMA, Bashara NM. Ellipsometry and Polarized light, Amsterdam: North Holland 1987.

[13] Fujiwara H. Spectroscopic Ellipsometry: Principles and Applications, New York: Wiley, 2007.

[14] Beaglehole D. Performance of A Microscopic Imaging Ellipsometer. Rev. Sci. Instrum. 1988; 59: 12-2557.

[15] Jin G, Jansson R, Arwin H. Imaging ellipsometry revisited: Developments for visualization of thin. Rev. Sci. Instrum. 1996;67: 8-2930.

[16] Neumaier KR, Elender G, Sackmann E. Merkel R. Ellipsometric microscopy. Europhys. Lett. 2000;49;1-14.

[17] Linke F, Merkel R. Quantitative Ellipsometric Microscopy at The Silicon–Air Interface. Rev. Sci. Instrum. 2005;76: 6-063701.

[18] Fukuzawa K, Yoshida T, Itoh S, Zhang H. Motion Picture Imaging of a Nanometer-thick Liquid Film Dewetting by Ellipsometric Microscopy with a Sub-μm Lateral Resolution. Langmuir 2008; 24: 20-11645.

[19] Fukuzawa K, Qingqing L, Tarukado T, Kajihara Y, Watanabe R, Itoh S, Zhang H. Novel Methods for Real-time Observation of Molecularly Thin Lubricant Films by Ellipsometric Microscopy: Application to Dewetting Observation. IEEE Trans. Magn. 2013; 49: 6-2530.

[20] Fukuzawa K, Miyata K, Yamashita C, Itoh S, Zhang H. Real-Time Observation of Molecularly Thin Lubricant Films on Head Sliders Using Rotating-Compensator-Based Ellipsometric Microscopy. IEEE Trans. Magn., in press.

[21] Johnson KL. Contact Mechanics. Cambridge, UK: Cambridge University Press; 1985, p.56-63.

[22] Hamrock BJ, Dowson D. Ball Bearing Lubrication. New York: John Willey & Sons, 1981.

[23] Hooke CJ. Elastohydrodynamic lubrication of heavily loaded contacts. J. Mech. Eng. Sci. 1977; 19: 4-149.

[24] Cameron A. Principle of Lubrication. Harlow, UK: Longman, 1966.

[25] Aspen DE. Bounds on Allowed Values of the Effective Dielectric Functions of Two-Component Composites at Finite Frequencies. Phys. Rev. B 1982; 25: 2-1358.

[26] Timoshenko S. Strength of Materials, Toronto: D. Van Nostrand, 1941.

Figure Captions

Fig. 1 Schematic setup for measuring lubricating film thickness by VEM: (a) setup and (b) magnified view around gap (region enclosed in blue line in (a)).

Fig. 2 Calibration of ellipsometric image intensity to film thickness: (a) RCE-based method, (b) piezo-based method. h_p is the difference between thickness measured by RCE-based and piezo-based methods. Blue and red lines represent data obtained by RCE- and piezo-stage-based methods, respectively.

Fig. 3 Relationship between ellipsometric image intensity and compensator angle. Areas numbered 1 to 16 indicate the integrals of the ellipsometric image intensity I_1 to I_{16}.

Fig. 4 Conversion curve from ellipsometric image intensity to film thickness. (a) Experimental results. Blue circles and red circles were obtained by RCE- and piezo-stage-based methods, respectively. (b) Comparison between experimental and theoretical curves. Black curve is a fitting curve shown in (a) for experiment. Red curve was theoretically obtained using Eqs. (2), (3), (7), and (8).

Fig. 5 Measured film thickness in static contact. Red dots show measured film thickness, and blue line shows film thickness predicted by Hertzian contact theory.

Fig. 6 Film thickness in sliding gaps measured by VEM: (a) contour map of film thickness at load of 1.7 mN and (b) that at 8.5 mN.

Fig. 7 Film thickness in sliding gaps measured by VEM at load of 1.7 mN. (a) Film profile at center line of Fig. 6(a) in x-direction (parallel to lubricant flow direction). (b) Film profile at center line of

Fig. 6 (a) in *y*-direction (normal to lubricant flow). Blue lines represent film thickness between plane and sphere as same diameter as metal-coated lens as a guide for the eye. Arrow shows direction of lubricant flow.

Fig. 8 Film profile in sliding gaps measured by VEM at load of 8.5 mN. (a) Film profile at center line of Fig. 6 (b) in *x*-direction (parallel to lubricant flow direction). (b) Film profile at center line of Fig. 6 (b) in *y*-direction (normal to lubricant flow). Blue lines represent film thickness between plane and sphere as same diameter as metal-coated lens as a guide for the eye. Arrow shows direction of lubricant flow.

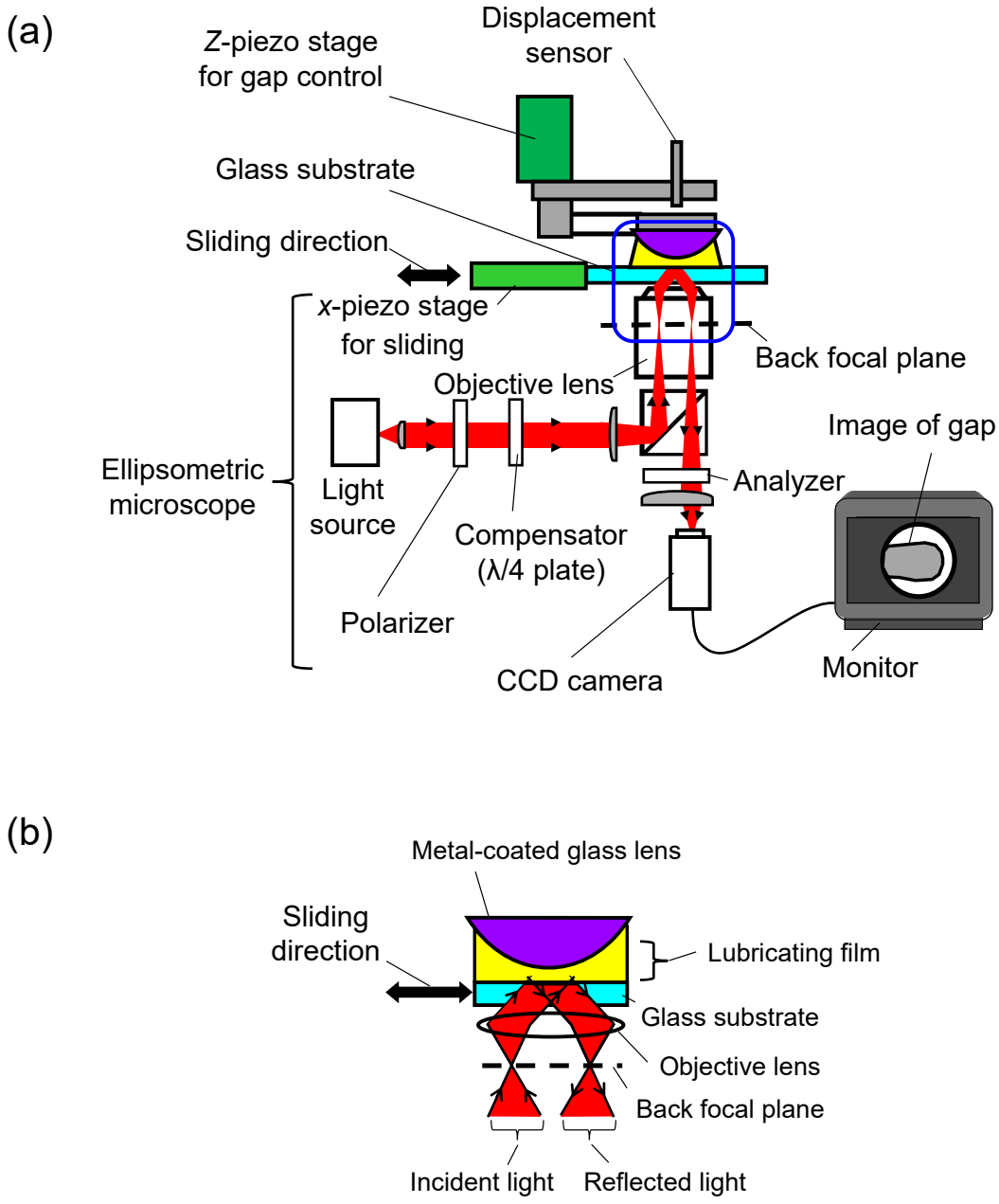
(a)
Z-piezo stage
for gap control
Displacement
sensor
Glass substrate
Sliding direction
x-piezo stage
for sliding
Back focal plane
Objective lens
Image of gap
Ellipsometric
microscope
Light
source
Analyzer
Compensator
(λ/4 plate)
Polarizer
CCD camera
Monitor
(b)
Metal-coated glass lens
Sliding
direction
Lubricating film
Glass substrate
Objective lens
Back focal plane
Incident light
Reflected light

Fig. 1

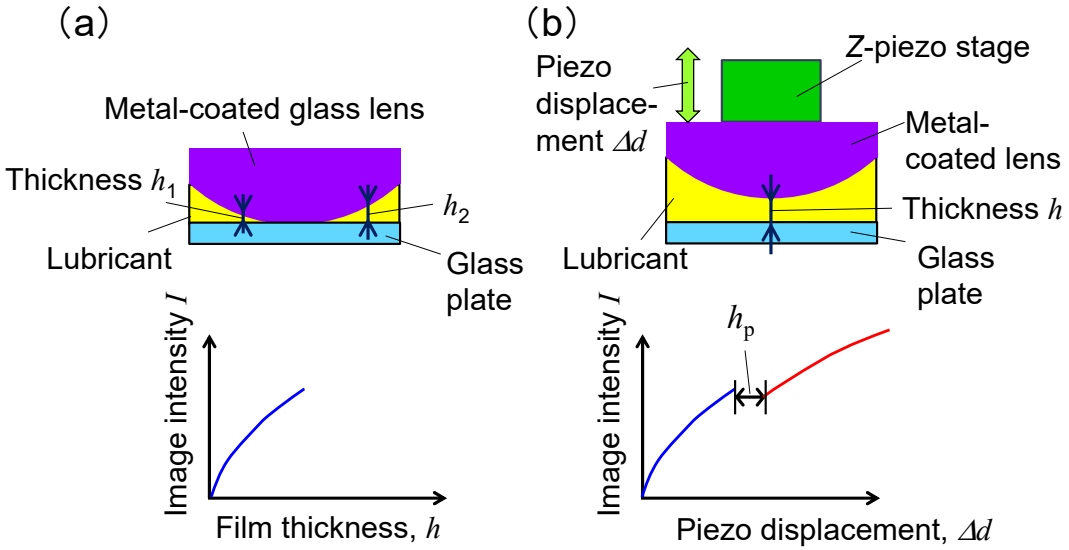
(a)
Metal-coated glass lens
Thickness h_1
h_2
Lubricant
Glass plate
Image intensity I
Film thickness, h
(b)
Piezo displace-ment Δd
Z-piezo stage
Metal-coated lens
Thickness h
Lubricant
Glass plate
h_p
Image intensity I
Piezo displacement, Δd

Fig. 2

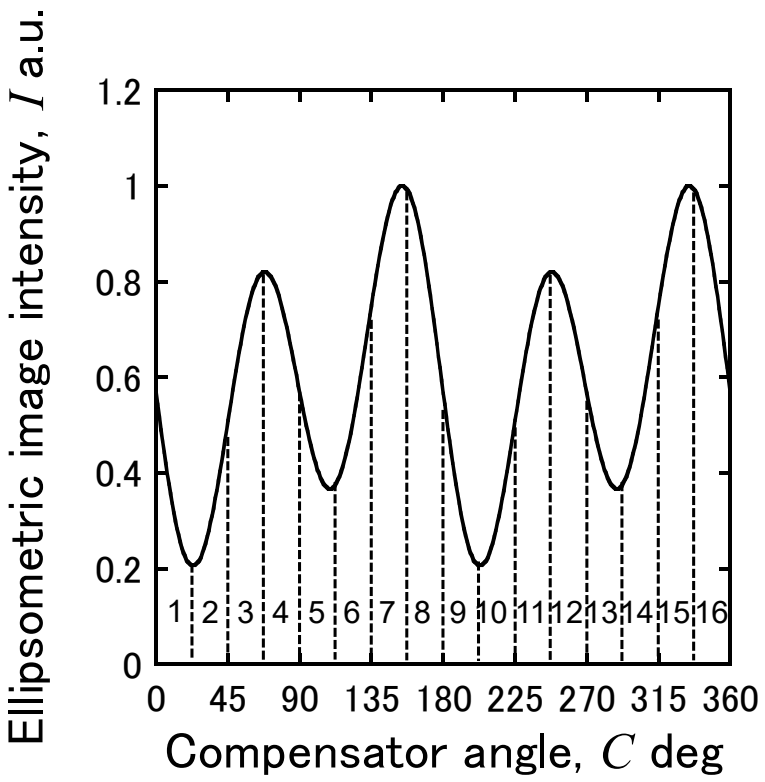
Ellipsometric image intensity, I a.u.
1.2
1
0.8
0.6
0.4
0.2
0
1 2 3 4 5 6 7 8 9 10 11 12 13 14 15 16
0 45 90 135 180 225 270 315 360
Compensator angle, C deg

Fig. 3

(a)

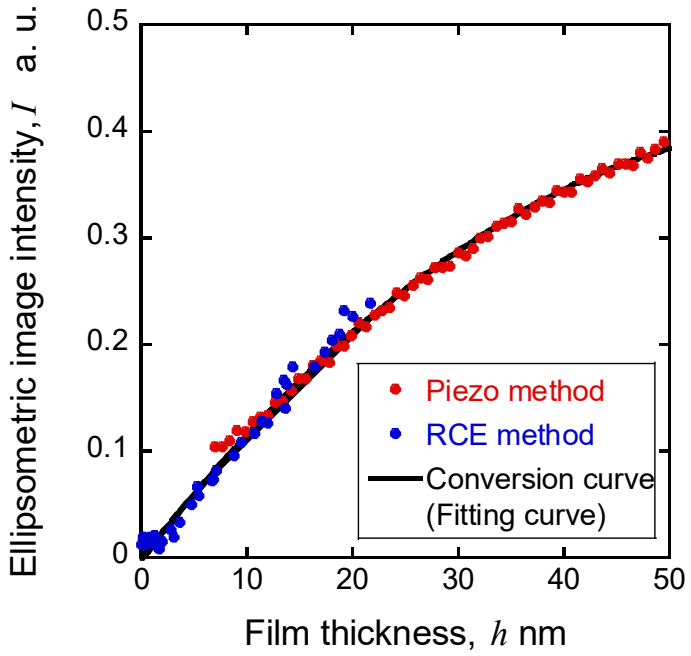
Ellipsometric image intensity, I a. u.
0.5
0.4
0.3
0.2
0.1
0
0
10
20
30
40
50
Film thickness, h nm
Piezo method
RCE method
Conversion curve
(Fitting curve)

(b)

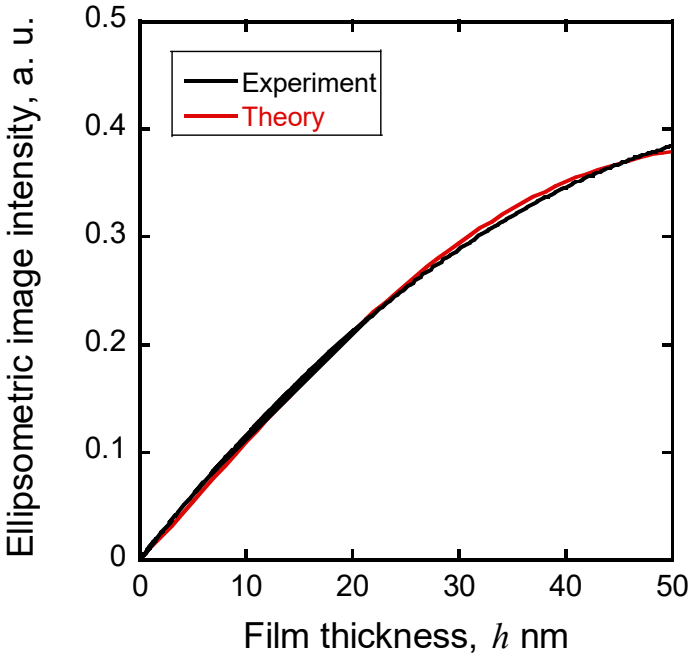
Ellipsometric image intensity, a. u.
0.5
0.4
0.3
0.2
0.1
0
0
10
20
30
40
50
Film thickness, h nm
Experiment
Theory

Fig. 4

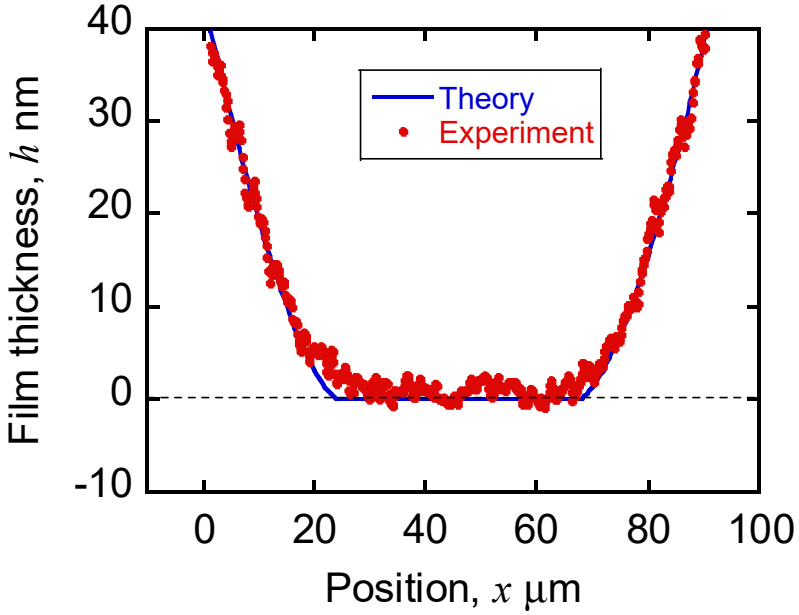
Theory
Experiment
Film thickness, h nm
Position, x µm
40
30
20
10
0
-10
0
20
40
60
80
100

Fig. 5

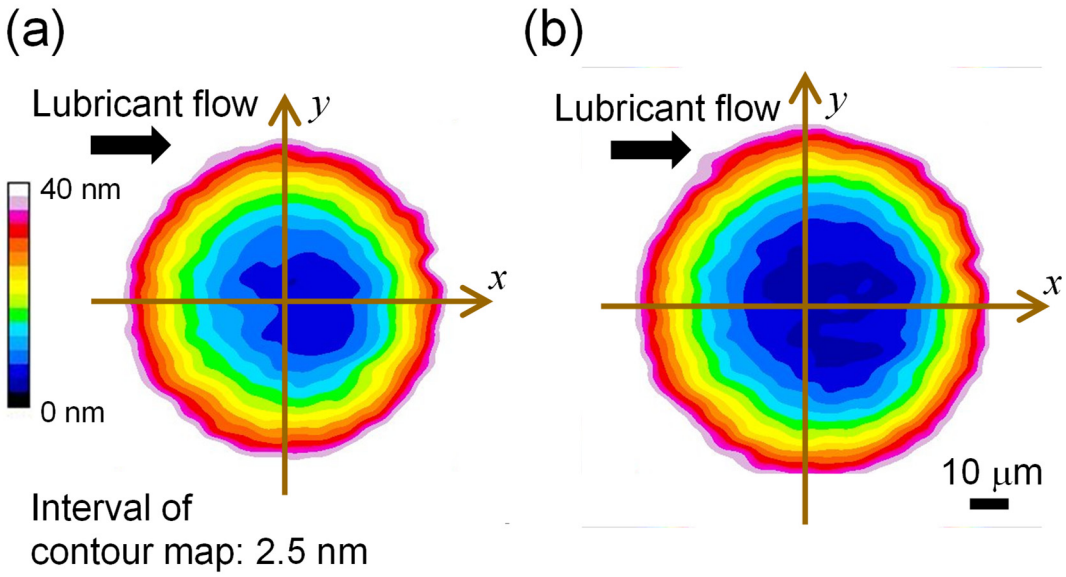
(a)
Lubricant flow
y
x
40 nm
0 nm
Interval of
contour map: 2.5 nm
(b)
Lubricant flow
y
x
10 μm

Fig. 6

(a)

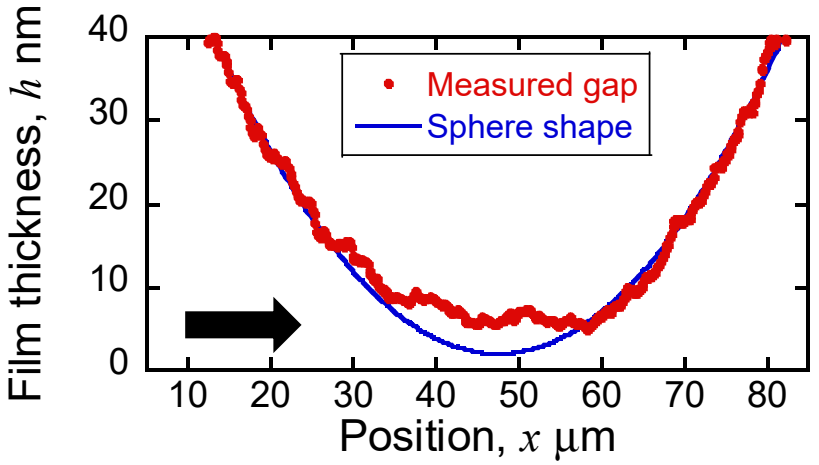
Film thickness, h nm
40
30
20
10
0
10
20
30
40
50
60
70
80
Position, x µm
Measured gap
Sphere shape

(b)

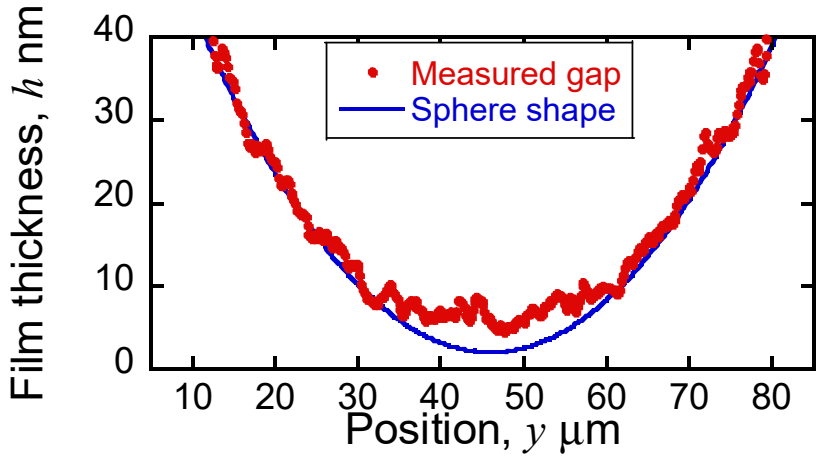
Film thickness, h nm
40
30
20
10
0
10
20
30
40
50
60
70
80
Position, y µm
Measured gap
Sphere shape

Fig. 7

(a)

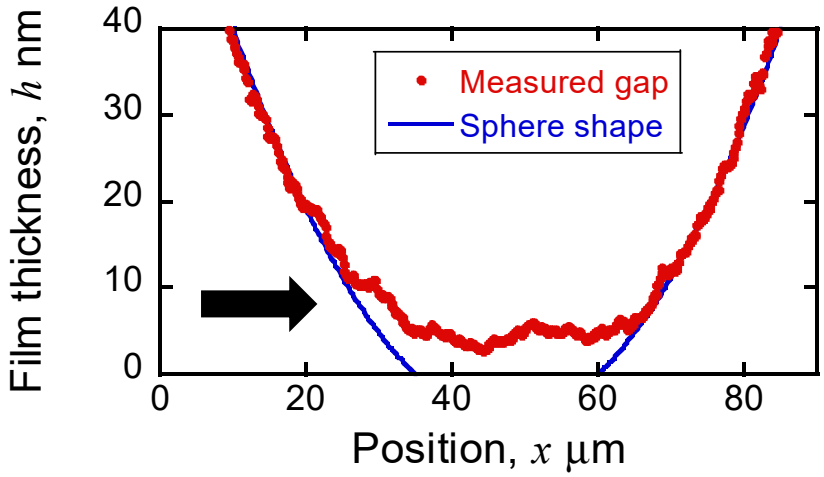
Film thickness, h nm
40
30
20
10
0
0
20
40
60
80
Position, x µm
Measured gap
Sphere shape

(b)

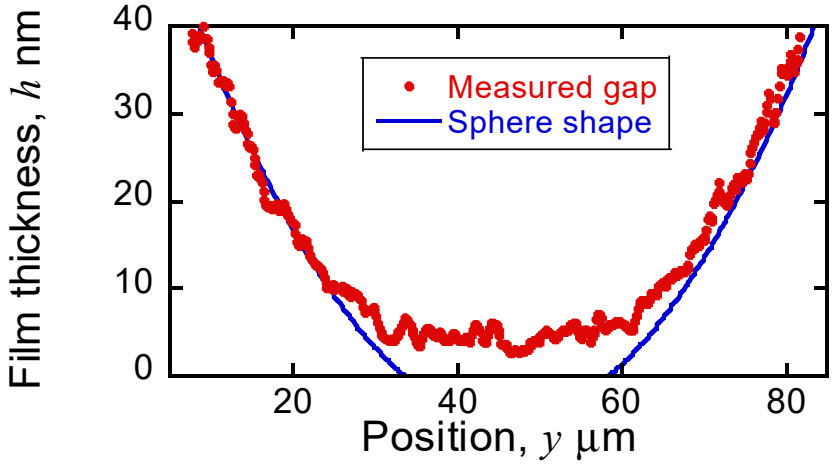
Film thickness, h nm
40
30
20
10
0
20
40
60
80
Position, y µm
Measured gap
Sphere shape

Fig. 8